Epilepsia, 54(4):667–677, 2013
doi: 10.1111/epi.12129

FULL-LENGTH ORIGINAL RESEARCH

Surface-based laminar analysis of diffusion abnormalities in cortical and white matter layers in neocortical epilepsy

***†Rajkumar Munian Govindan, *†Eishi Asano, *†Csaba Juhasz, *†Jeong-won Jeong, and *†Harry T. Chugani**

*** Departments of Pediatrics; and † Neurology, Children's Hospital of Michigan, Detroit Medical Center, Wayne State University School of Medicine, Detroit, Michigan, U.S.A.**

Summary

Purpose: Microstructural alterations seen in the epileptic cortex have been implicated as a cause and also result of multiple seizure activity. In the present study, we evaluated water diffusion changes at different cortical thickness fractions and in the underlying white matter of the epileptic cortex and compared them with electrographically normal cortex and also with corresponding cortical regions of healthy controls.

Methods: We selected 18 children with normal magnetic resonance imaging (MRI) who underwent two-stage epilepsy surgery to control seizures of neocortical origin, and compared their MR images with those of 18 age-matched healthy controls. First, delineation of the gray-white and gray-pial intersection surfaces was performed on high-resolution volumetric T1 MR images. Using the delineated surfaces as reference, diffusion values were measured at different cortical thickness fractions and in the underlying white matter at various depths, using diffusion tensor imaging (DTI). Cortical regions representing seizure onset and electrographically normal cortex were differentiated by electrocorticography in the epilepsy patients.

Key Findings: We observed different patterns of diffusion abnormalities in both the seizure onset and electrographically normal cortical regions when compared to healthy controls. In the seizure-onset regions, a marked *increase* in diffusivity was noted in the cortical gray matter, and this increase was most pronounced in the outer fraction of the gray matter. Similarly, increased diffusivity was noted in the white matter underlying the epileptic cortex. The electrographically normal cortex, in contrast, showed *decreased* diffusivity in inner and middle cortical fractions compared to the controls. The white matter underlying the electrographically normal cortex did not show any difference in diffusivity between the children with epilepsy and controls. Finally, both the cortical gray matter and the underlying white matter regions showed decreased anisotropy in epileptic as well as electrographically normal regions when compared to controls.

Significance: Our results suggest specific patterns of diffusion changes in the cortical fractions and the underlying white matter of the epileptic region compared to electrographically normal and normal control regions. The abnormal increase in diffusivity of the superficial cortex might be associated with microstructural abnormalities commonly seen in layers II through IV of epileptic cortex. Such combined use of a high-resolution structural image to extract the laminar diffusion values, which are highly sensitive to microstructural alterations, could be of clinical value in localizing epileptogenic cortex.

KEY WORDS: Epilepsy, Diffusion, Surface, Seizure, DTI.

Neural tissue is highly organized with complex architectural patterns of cell alignment and extending processes. This unique architectural complexity creates several cellular and subcellular and intercellular compartments and, depending on the composition and permeability of these compartments, diffusion of water molecules is partially restricted and exhibits unique diffusion characteristics (Moseley et al., 1990; Beaulieu, 2002). Measurement of these water diffusion characteristics using diffusion magnetic resonance imaging (MRI) techniques provides an indication of the structural integrity of neural tissue. Using such imaging techniques, appreciable changes in water diffusion were noted in brain tissue at risk for neuronal damage in a rat model of status epilepticus; such changes were not apparent using conventional MRI methods, for example, T_1 or T_2 images (Engelhorn et al., 2007). This improved sensitivity to detect structural changes has been applied in several human neurologic disorders, including epilepsy (Rugg-Gunn et al., 2001; Mukherjee et al., 2008; Yu & Tan, 2008).

In epilepsy, several diffusion MRI studies have demonstrated abnormalities involving gray as well as white

Accepted January 7, 2013; Early View publication February 28, 2013.
Address correspondence to Harry T. Chugani, Department of Pediatric Neurology/PET Center, Children's Hospital of Michigan, 3901 Beaubien Blvd, Detroit, MI 48201, U.S.A. E-mail: hchugani@pet.wayne.edu; mgrajkumar45@gmail.com
This study was performed with approval from the Wayne State University Human Subjects Research Committee.

matter extending beyond the electroencephalography (EEG)–defined epileptic focus (see review, Duncan, 2008). However, application of diffusion MRI in the identification of cortical regions involved in the generation and propagation of epileptic activity has been difficult. At least part of this difficulty is because seizures are functional disturbances often originating from normal appearing viable neural tissue. Although in most cases of epilepsy, some microstructural abnormalities may be associated with the seizure activity (Woermann et al., 1998), these structural abnormalities are often too subtle to cause a noticeable signal change, even with the highly sensitive diffusion MRI scans. In addition, seizure activity itself may cause tissue alterations that are often noted in diffusion scans acquired in the ictal or the immediate postictal phase; however, these positive diffusion signal changes are highly variable depending on time since seizure onset, propagation and spread along the epileptic network, seizure intensity, and probably other less well-understood factors (Yu & Tan, 2008).

In the white matter, diffusion is highly anisotropic, thus providing improved sensitivity to observe even minor structural changes (Beaulieu, 2002). This diffusion property, combined with tractography and other tract analysis methods, has increased our understanding of the diffusion changes in epilepsy (Duncan, 2008). Using tractography in children with chronic temporal lobe epilepsy, extensive diffusion abnormalities were noted in the ipsilateral as well as contralateral temporal and extratemporal lobe white matter tracts (Govindan et al., 2008). Duration of the epilepsy also showed significant correlation with the diffusion parameters. Similar findings in other studies suggest that these white matter abnormalities are possibly common to all regions of the epileptic brain (i.e., widespread) and may not provide precise localization for the epileptogenic region (Concha et al., 2005, 2007). Therefore, despite improvements in the sensitivity and analysis of diffusion images, our ability to isolate epileptic cortex using this approach has been difficult.

In the epileptic cortex, it has been demonstrated that the pathologic changes (when present) are most prevalent in cortical layers II through IV where the cortical neurons are most concentrated (Farrell & Vinters, 1997). Therefore, a method with the ability to measure the diffusion values from this particular zone of the cortex may show more specific diffusion findings and thus provide seizure focus localization data. In addition, because axons arise from the body of the cortical neuron and descend to the white matter, the white matter zone immediately underneath the epileptic cortex will contain axons mostly arising from the overlying cortex with minimal crossing (or contamination) from distant or adjacent groups of axons. Therefore, an analysis method that isolates this superficial region of the white matter may also provide information unique to the epileptic cortex.

Measuring the diffusion values from such narrow cortical and white matter regions, however, is likely to be difficult. Nevertheless, despite the low spatial resolution of diffusion MR images, several tractographic and white matter analysis methods have applied protocols to delineate or segment the white matter tracts, and these have been reasonably successful (Govindan et al., 2008). In particular, the white matter analysis method designed by Smith et al. (2006; tract based spatial statistics, TBSS) used the median portion of the white matter tract as a reference skeleton and measured the maximal diffusion values along the perpendicular width of the tract. Using such reference points has greatly improved our ability to measure and compare smaller regions. With the concurrent use of high-resolution structural T_1 images, precise delineation of cortical surfaces (gray–white and gray–pial interface) is now possible and thickness of the cortex can be measured with reasonable accuracy (Fischl & Dale, 2000).

In an attempt to measure diffusion values from these narrow cortical and subcortical white matter zones, we performed rigorous spatial alignment of diffusion images to a high-resolution structural image and used the gray–white and gray–pial interface surfaces as reference points to measure the diffusion values in the adjacent cortical and subcortical white matter regions. In addition to the evaluation of apparent diffusion coefficient (ADC) of water in these regions, we also analyzed the fractional anisotropic index (FA). Finally, we used subdural electrocorticography data as the gold standard to identify seizure onset and normal cortex and retrospectively compared the diffusion values in these regions to the corresponding regions of controls. We hypothesized that ADC and FA would differ, at the narrow cortical and subcortical white matter zones, between electrographically defined seizure focus and normal cortex.

Methods

Subjects

We studied 18 children (mean age 8.3 ± 5.3 years, range 2.2–19.7 years) diagnosed with intractable epilepsy who underwent two-stage epilepsy surgery (i.e., implantation of subdural electrodes followed by cortical resection) for control of their seizures. All the children underwent presurgical diffusion MRI along with the routine clinical scans, and no apparent lesions were identified by routine radiologic examination. Following extensive discussions, based on the clinical, imaging (including positron emission tomography), and scalp electrographic data, the side and the location of the subdural electrodes to be placed were decided (described in detail in Asano et al., 2009). After 2 to 5 days of subdural electrographic recordings, the presumed seizure focus was determined and surgical resection was performed. In 10 subjects this procedure was performed on

Table 1. Epileptic group's profile

ID	Age (years)	Epileptic side	Surgical resection performed
1	10.63	Right	Multiple subpial transsection
2	17.75	Left	Temporal resection
3	2.24	Left	Hemispherectomy
4	19.73	Right	Parietal resection
5	8.53	Right	Subtotal hemispherectomy
6	13.91	Right	Temporal resection
7	13.59	Left	Temporal resection
8	4.91	Left	Frontal resection
9	3.01	Left	Subtotal hemispherectomy
10	10.29	Left	Temporal resection
11	2.51	Left	Subtotal hemispherectomy
12	3.75	Left	Temporoparietal-occipital resection
13	3.56	Left	Temporo-parietal-fronto-occipital resection
14	5.55	Left	Hemispherectomy
15	6.03	Right	Frontal resection
16	10.88	Right	Subtotal hemispherectomy
17	8.05	Right	Frontal resection
18	2.41	Right	Subtotal hemispherectomy

the left hemisphere and in eight subjects on the right hemisphere (Table 1). Eighteen normal healthy children who had undergone diffusion tensor imaging (DTI)-MRI scans were selected as control subjects (mean age 7.8 ± 4.6, range: 4–20 years) and paired age-wise with the epileptic children. In all our control subjects consent was obtained from both the subject and parent/guardian; sedation was not used. This study was performed with approval from the Wayne State University Human Subjects Research Committee.

MRI acquisition protocol

All participants were scanned on a GE 3T Signa scanner (GE Healthcare, Milwaukee, WI, U.S.A.) using an 8-channel head coil. The MRI acquisition included the following series: (1) 3-dimensional structural MRI scan of the brain using a T_1-weighted inversion recovery fast spoiled gradient recall (FSPGR) sequence designed to optimize the tissue contrast between gray and white matter (repetition time/echo time/inversion time 6.2/2.5/450 msec; field of view 250 × 250 mm^2, and slice thickness of 1.2 mm). (2) Diffusion weighted images were acquired in the axial plane with diffusion sensitization gradients applied at 55 noncollinear directions (b value 1,000 s/mm^2). In addition, T2-weighted image (B0) was acquired at b value = 0 s/mm^2 and used for a reference image to normalized the diffusion attenuation at individual gradient images. All diffusion acquisitions were at repetition time/echo time 9,000–11,000/80 msec, field of view 220 × 220 mm^2, 38–44 slices; 2.5-mm thickness with zero gap, acquisition matrix 128 × 128, reconstruction matrix 256 × 256, and number of acquisition = 1. Double radio frequency refocusing pulses and parallel imaging capability were applied to reduce eddy current and geometric distortion artifacts derived from echo-planar imaging.

Diffusion parameter calculation

The tensor calculation of the diffusion images was performed using DTISTUDIO software (Jiang et al., 2006). The T_1-weighted (SPGR) structural image, native T_2-weighted (B0) image, and the images derived from this tensor calculation: apparent diffusion coefficient (ADC) and fractional anisotropy (FA) images were saved and transferred to a Linux-based workstation for further processing. Following this, the brain extraction of the diffusion images; segmentation and surface delineation of the structural T_1 image; registration, fractionation, and selection of epileptic and normal cortical regions were performed as explained below.

Brain extraction

This initial step involved the extraction of the brain matter from the B0 images of all the subjects using the Brain Extraction Tool (BET; Smith, 2002) available with the FSL software (FMRIB Software Library, Oxford, United Kingdom); a fractional intensity threshold of 0.35 was used for this step. Using the brain extracted B0 image as a mask, the extra-brain tissue regions from the diffusion tensor images were removed.

Segmentation and surface reconstruction

Using the FREESURFER software (http://surfer.nmr.mgh.harvard.edu/), separation of the cortical hemispheres, segmentation of each hemisphere into gray and white matter, and reconstruction and delineation of the gray–white matter (G-W) and gray-pial (G-P) interface surfaces for each of the cortical hemispheres were performed using the T_1-weighted SPGR structural image (described in detail at Dale et al., 1999; Fischl et al., 1999a, 2002).

Registration

Following this isolation of the brain from the raw high-resolution structural image, the brain extracted FA image of the subject was spatially registered on to the brain-extracted structural brain image (structural image prior to gray–white segmentation) using a simple rigid body (six degrees of freedom) registration and then followed by a rigorous nonlinear image registration (FNIRT; FSL, used in procedures such as TBSS where strict spatial alignment of diffusion images are required [Smith et al., 2006]). The spatial transformation protocols for this transformation (two-dimensional [2D] transformation matrix and the warp image) were saved and applied to the other diffusion parameters (ADC and FA) images (Fig. 1). After this registration procedure, all the diffusion parameter images were resampled to the structural image space for further analysis. Because the T_1 and the FA images have similar image intensity and contrast profile across the gray and white matter structures, we chose the FA image for the diffusion-to-structural registration.

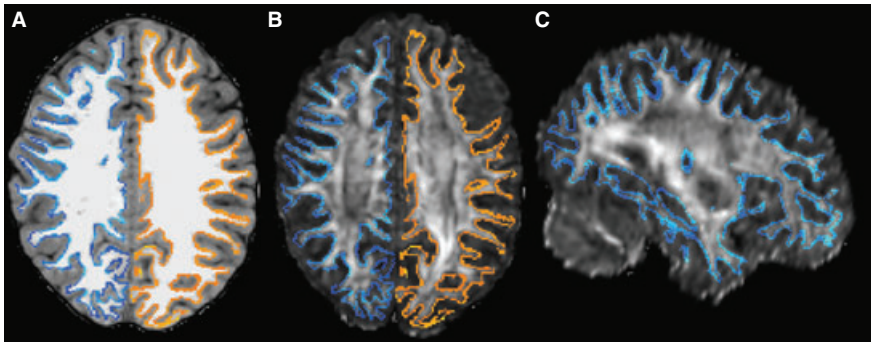

Figure 1.
Shows the (**A**) structural T_1, (**B**) registered FA, and (**C**) registered FA (sagittal) images with the delineated gray–white interface surface (blue and orange) following the nonlinear registration procedure.
Epilepsia © ILAE

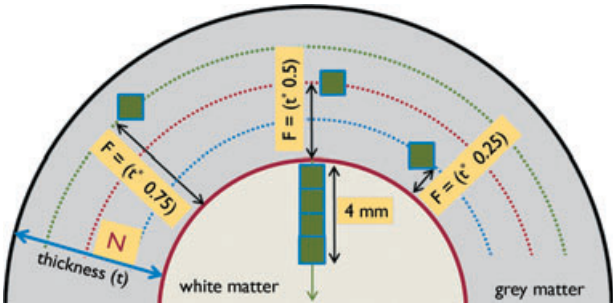

Figure 2.
Shows the scheme of method used to measure the diffusion values using the gray–white and gray–pial interface surface. N: normal vector from the vector point of the surface, t: thickness of the cortex at the vertex point. Red line: gray–white interface surface, Black line: gray–pial interface surface, F: fractionation variable, Green square: diffusion values measurement space.
Epilepsia © ILAE

Laminar fractionation of the gray and white matter

Subsequently, the reconstructed G-W and the G-P interface surfaces of the structural image were used as the boundaries of the gray and the white matter, and several new surface images were created using these surfaces as references. In the cortex, at each surface point, the distance between the G-W and G-P surfaces was considered as the cortical thickness (t). The average diffusion measure across the thickness of cortex was measured (cortical average). From cortical thickness (t), the fractional thickness distance ($0 \times t$, $0.25 \times t$, $0.5 \times t$ and $0.75 \times t$) was calculated. By applying the fractional thickness distance ([positive] $0 \times t$, $0.25 \times t$ and $0.5 \times t$) along the normal vectors (pointing outward) of the reference G-W surface, the diffusion values were measured (Fig. 2) for that cortical fraction and then projected onto new surface images (gray–white zone, inner-, middle- fractions, respectively) for each of the registered diffusion parameter images. To minimize the effect due to the convergence and divergence of normal vectors of the curved surfaces, we used the G-P surface (instead of G-W) to measure the diffusion value from the outer fraction of the cortex (with [negative] $-0.25 \times t$). In the white matter, new surfaces were created with the projected values from the white matter at a fixed depth (1, 2, …, 5 mm) from the G-W surface with the distance measured along the normal vectors (pointing inward) of the reference G-W surface.

Region of interest analysis

Following the reconstruction of the surfaces, the pial (G-P) surface of the abnormal hemispheres of the epileptic subjects was displayed using the "tksurfer" tool (Dale et al., 1999). Subdural electrode locations were superimposed on the individual three-dimensional (3D) surface MR image as previously described (Alkonyi et al., 2009). Along with the clinical electrocorticographic data, regions of the cortex with seizure onset and electrographically normal cortex (defined as the sites not showing seizure onset or interictal spike activity) were identified by the clinical neurophysiologist blinded to the results of DTI analysis (Asano et al., 2009). Regions were drawn on the pial (G-P) surface directly underlying all the electrodes showing seizure onset and normal electrographic findings. These regions were then projected onto the laminar surfaces created earlier and the diffusion parameter values from these regions were noted. In controls, similar calculation, segmentation, registration, and laminar fractionation procedures were performed to create the laminar surfaces. From each of the epileptic subjects, all the regions were transformed to the corresponding cortical regions of the age-matched control pair following a surface-based registration process (Fischl et al., 1999b). These regions were then projected onto the diffusion surfaces and the parameter values were noted.

Statistical analysis

Repeated measures analysis of variance was performed with group, electrographic type, and cortical fractions (or) white matter layers as factors. Analysis was performed for both of the tensor parameters (ADC and FA) separately. For the cortical average values, group and electrographic type was used as factors. Paired *t*-test analysis for difference between the ages of both the group (epileptic and control) showed no significant age difference between the groups

(p = 0.56). All statistical analyses were performed using SPSS version 20 (IBM, Armonk, New York, U.S.A.).

Results

ADC

In the cortex, for the cortical average values the two-way interaction between the group and the electrographic type was significant (p = 0.001). In the seizure-onset regions, the mean ADC values of the whole cortical thickness was significantly higher when compared to controls (p = 0.003), whereas the mean ADC value from the electrographically normal regions was decreased compared to the controls (p = 0.058) (Fig. 3).

Furthermore, the three-way interaction between the group, electrographic type and cortical fractions was significant (p = 0.014). In seizure-onset regions, the ADC of all four cortical fractions were significantly (p < 0.01) higher compared to the normal regions within the epileptic group (Fig. 4). A specific and significantly (p = 0.001) marked increase in ADC was noted in the outer fraction (and middle fraction less marked but significant; p = 0.047) of the seizure-onset regions compared to the corresponding regions of the controls as well as the electrographically normal regions (p = 0.001) (Fig. 4). In the electrographically normal regions, the ADC values were significantly (p < 0.003) lower in the inner and middle fractions (and apparently lower in the gray–white zone (p = 0.089)) as compared to the controls (Fig. 4).

In the white matter, the two-way interaction between the group and layers was significant (group × layers; p = 0.034). The seizure-onset regions showed increase in ADC values compared to the electrographically normal cortex as well as to the corresponding regions of the controls at all the white matter depths. The increase in the ADC values was more marked and significant in the deeper (5, 4, and 3 mm) layers and less marked in the superficial (2 and 1 mm) layers.

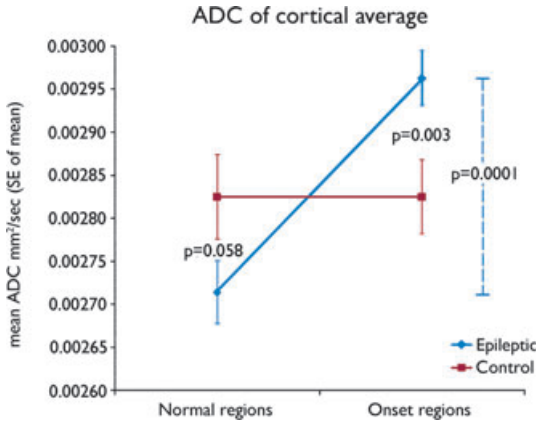

Figure 3.
Plot shows the mean ADC values of the whole cortical thickness in the electrographically normal and seizure-onset regions of the epileptic subjects. The control values represent the mean ADC values from the corresponding regions of the control subjects. The two-way interaction between the groups (epileptic and control subjects) and the electrographic types (normal and onset) was significant (p = 0.001).
Epilepsia © ILAE

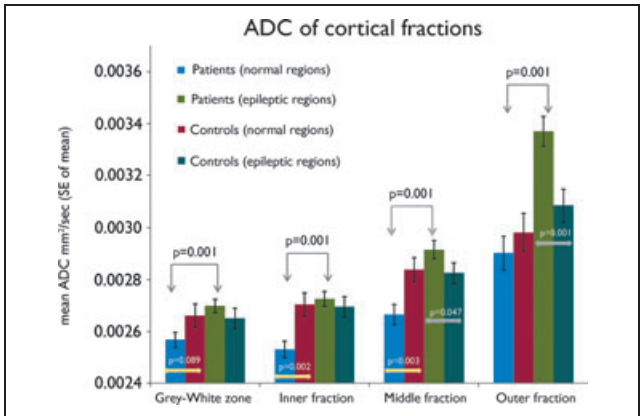

Figure 4.
Chart showing the mean ADC values of the cortical fractions in the electrographically normal and seizure-onset regions of the epileptic subjects. The control values represent the mean ADC values from the corresponding regions of the control subjects. The three-way interaction between the groups (epileptic and control subjects), electrographic types (normal and onset), and cortical fractions were significant (p = 0.014). The partial volume effect from CSF can be noted with an exponential increase of ADC values from deeper to superficial cortical fractions.
Epilepsia © ILAE

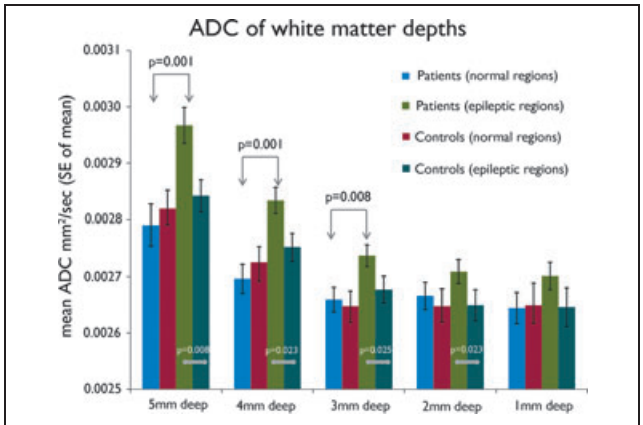

Figure 5.
Chart showing the mean ADC values of the underlying white matter at various depths (mm) from the gray–white surface in the electrographically normal and seizure-onset regions of the epileptic subjects. The control values represent the mean ADC values from the corresponding regions of the control subjects. The two-way interaction between the groups (epileptic and control subjects) and white matter depths was significant (p = 0.034), as well as between electrographic types (normal and onset) and cortical fractions (p = 0.014).
Epilepsia © ILAE

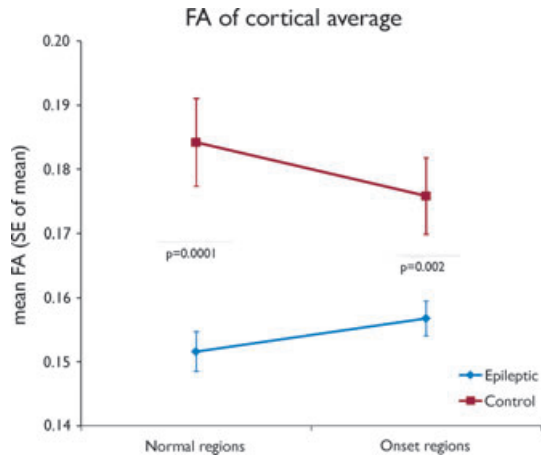

Figure 6.
Plot shows the mean FA values of the whole cortical thickness in the electrographically normal and seizure-onset regions of the epileptic subjects. The control values represent the mean FA values from the corresponding regions of the control subjects. The interaction between the groups (epileptic and control subjects) was significant ($p = 0.001$).
Epilepsia © ILAE

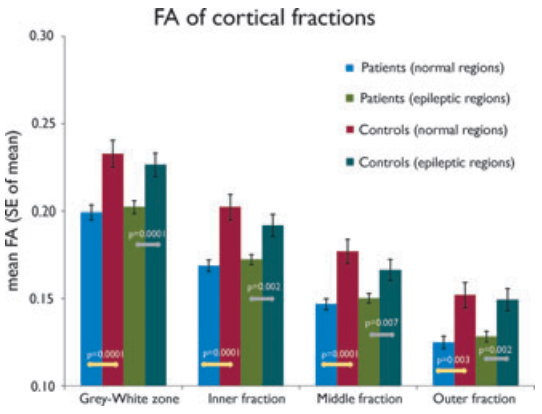

Figure 7.
Chart showing the mean FA values of the cortical fractions in the electrographically normal and seizure-onset regions of the epileptic subjects. The control values represent the mean FA values from the corresponding regions of the control subjects. The group interaction between the groups (epileptic and control subjects) was significant ($p = 0.0001$). The partial volume effect from the CSF can be noted with a progressive decrease of FA values from deeper to superficial cortical fractions.
Epilepsia © ILAE

In contrast, the ADC values from the electrographically normal regions of the epileptic group were not different from the corresponding region of controls in all depths (Fig. 5).

FA

There was no significant difference in FA between seizure onset and electrographically normal (Fig. 6). Nonetheless, in the cortex, for the cortical average values the interaction between the groups was significant ($p = 0.0001$). The mean FA values from both the seizure onset regions and the electrographically normal regions were decreased in the epileptic group compared to the control groups ($p < 0.002$) (Fig. 6).

For both the cortical fractions and the white matter layers, the group interaction between the patients and the controls was significant (group; $p = 0.0001$). The mean FA values from all (both seizure-onset and electrographically normal) regions of the epileptic group were significantly lower in all the cortical fractions and the white matter depths compared to the controls (Figs. 7 and 8). In addition, the mean FA values from the seizure-onset regions were not different from the electrographically normal regions of the epileptic group (Figs. 6, 7, and 8).

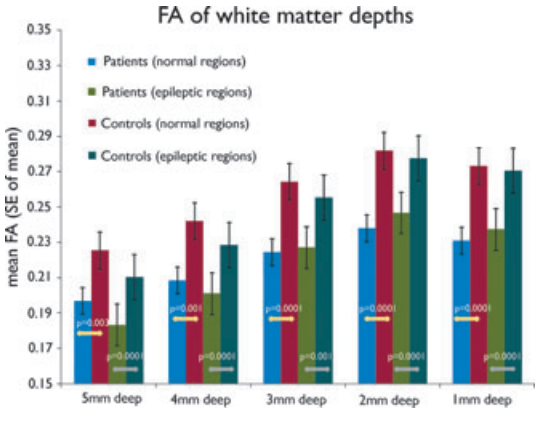

Figure 8.
Chart showing the mean FA values of the underlying white matter at various depths (mm) from the gray–white surface in the electrographically normal and seizure-onset regions of the epileptic subjects. The control values represent the mean FA values from the corresponding regions of the control subjects. The group interaction between the groups (epileptic and control subjects) was significant ($p = 0.0001$).
Epilepsia © ILAE

Discussion

The major findings of the present study are that children with intractable epilepsy show different patterns of diffusion abnormalities in both the epileptic and electrographically normal cortical regions when compared to controls. In the epileptic regions, a marked increase in diffusivity was noted in the cortical gray matter, and this increase was most pronounced in the outer segment of the gray matter. Similarly, increased diffusivity was noted in the white matter underlying the epileptic cortex. The electrographically normal cortex of patients, in contrast, showed decreased diffusivity in the inner and the middle cortical fractions com-

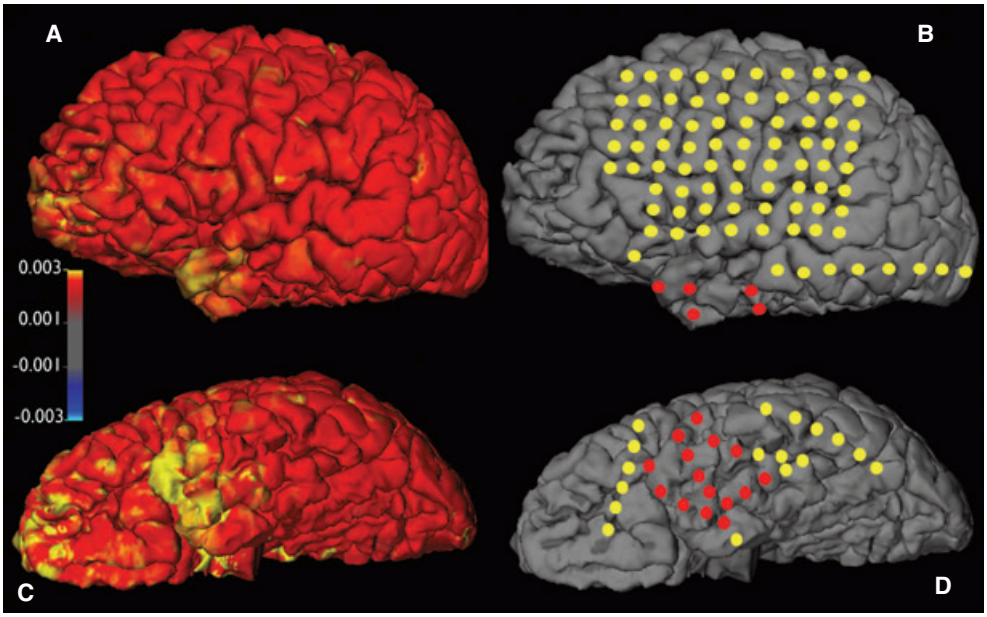

Figure 9.
Shows the diffusion abnormalities and the seizure-onset zone defined by intracranial electrocorticography. The ADC values were measured from the underlying white matter (at 2 mm depth from the gray–white interface) and projected on to the pial surface of the left cerebral hemisphere. The red circles represent the subdural electrode, which showed that seizure onset and yellow circles represent electrode not showing seizure onset or interictal spike activity. The seizure-onset zone in the left temporal pole region showed increased ADC values. Left anterior orbitofrontal region also showed increased ADC values, but this region was not evaluated. (**A**, **B**) lateral surface. (**C**, **D**) Inferior surface.

pared to normal controls. The white matter subjacent to electrographically normal cortex did not show any difference in diffusivity between the epileptic children and controls. Finally, both the cortical gray matter and the underlying white matter regions showed decreased anisotropy in epileptic as well as electrographically normal regions when compared to controls.

Diffusion abnormalities in the epileptic cortex

In human cerebral cortex the average thickness of the cortical gray matter averages approximately 3 mm. The cortex is thinner in the occipital lobe (2.5 mm) and thicker in the frontal and temporal lobes (3–4 mm) (Fischl & Dale, 2000). Within the gray matter, the neural tissue has a laminar pattern, with a variable clustering of neurons in layers I through VI. Based on estimates of the thickness of these individual layers from histologic methods, the sampling of diffusion values of the fractionated cortical layers (outer, middle, and inner) corresponds to the group of cortical layers (L I–II–III), (L III–IV–V) and (L V–VI), respectively (Smiley et al., 2012; Williams et al., 2012). In our findings, the abnormal increase in diffusivity noted specifically in the outer cortical fraction of the epileptic cortex corresponds to the superficial cortical layers (L I–II–III). This finding in the superficial cortical fraction is in agreement with other studies using high-resolution imaging or histopathologic methods (Garbelli et al., 2011). In addition, a significant, but milder, increase in diffusivity was noted in the middle cortical fraction; this increased diffusivity might be due to the extension of the thicker layer III into the middle cortical fraction. Similarly, in the underlying white matter regions, increased diffusivity was noted only under the epileptic cortical regions and not under electrographically normal cortex. Because the pyramidal neurons from the superficial cortical layers project their axons to distant sites through the underlying white matter, the increased diffusivity in white matter subjacent to epileptic cortex might be related directly to the abnormality seen in the outer (superficial) cortical fraction (layers (L II–III)).

Abnormality in the nonepileptic cortex

An interesting observation noted in the present study was that the decrease of ADC values was seen only in the normal regions of the inner and middle cortical fractions when compared to both epileptic regions and the corresponding regions of the controls. Such decreases were not seen in the epileptic cortex. Because the inner layers (L V–VI) of the cortex are strongly connected to subcortical structures (thalamus and basal ganglia), it is tempting to speculate that this decrease in ADC could be related to compensatory mechanisms (e.g., surround inhibition) to restrict the epileptic activity.

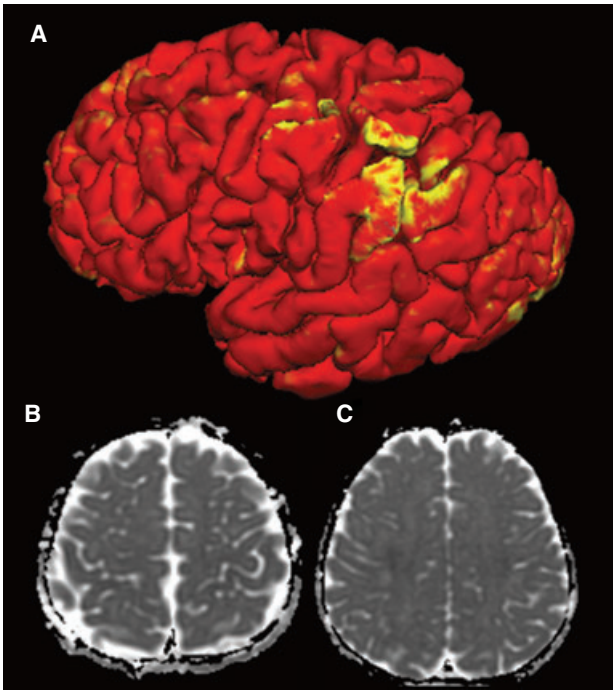

Figure 10.
An explicit diffusion abnormality in the dorsal surface of the left parietal cortex (**A**); this abnormality is not appreciated in the conventional transaxial slices (**B**, **C**) upon visual inspection. In the conventional approach, subtle diffusion changes present in a narrow cortical layer are typically missed because the abnormal diffusion signal is mild and there is no clear normal reference tissue region. Our surface-based method not only measures the diffusion values from narrow cortical fractions but also improves the sensitivity for detection by displaying the important reference values in a single surface. The ADC values were sampled at the outer cortical fraction and projected to the pial surface for display.

Global loss of anisotropy

Despite being highly sensitive to white matter changes, the FA values were decreased to the same extent in both the epileptic as well as the normal white matter regions of the patients compared to normal controls (Fig. 8). Similar decreases in the FA values were also noted in gray matter regions (Figs. 6 and 7). Indeed, these findings are consistent with several reports of similar widespread decreases in FA seen in epileptic subjects (Concha et al., 2005; Govindan et al., 2008; Duning et al., 2010).

Isolation of the epileptic cortex

The potential capability of diffusion MRI to demarcate epileptic cortex has been discussed in several previous studies (Rugg-Gunn et al., 2001; Konermann et al., 2003; Guye et al., 2007; Roberts, 2011). The present study lends further support to this claim by demonstrating contrasting patterns of diffusion abnormalities between epileptic and nonepileptic as well as normal cortex. Our findings which show combinations of diffusion abnormality with increased ADC values of the outer cortical fraction and the underlying white matter, and also the absence of decreased ADC of the inner cortical fractions, could provide an imaging biomarker to improve the accuracy in detecting the epileptic cortex.

In a previous study using a voxel-wise comparison method, the interictal diffusion data showed increased ADC in the seizure-onset zone as well as in more remote regions possibly involved in the seizure propagation network (Guye et al., 2007). Such diffusion abnormalities beyond the epileptic-onset zone would reduce our specificity in localizing the epileptic focus. In the present study, because we restricted our analysis to regions with subdural electrode coverage, we cannot rule out the possibility of sampling error, thus missing diffusion abnormalities at distant sites in the epileptic network. However, since the pathomechanism of abnormal electrical activity in the seizure-onset zone and in the propagation network regions are different, we can expect some differences in the characteristics (across fractions) and the magnitude of the diffusion abnormalities between these locations. In the seizure-onset zone, neuronal loss and gliosis are often found due to the repeated effects of seizures; therefore, more abnormal findings are expected in the outer cortical fractions and the underlying white matter regions of the onset zone. However, a larger and more comprehensive study with measurements from clearly demarcated (onset and propagation network) regions might provide better understanding of the diffusion differences between the onset and the propagation network regions.

Interpreting the surface-based diffusion data

In addition to showing the diffusion abnormalities, this study has also demonstrated the usefulness of the surface-based analysis method in measuring as well as visualizing the diffusion data (Fig. 9). In conventional radiology, the diffusion images are visually inspected on a slice by slice basis. In that clinical approach, subtle diffusion changes present in a narrow cortical layer are typically missed because the abnormal diffusion signal is mild and there is no clear normal reference tissue region. Moreover, the cerebrospinal fluid (CSF) that lies immediately adjacent to the outer cortical gray matter significantly confounds and masks abnormal diffusion changes close to the CSF rendering it difficult to identify subtle abnormal diffusion signals. In this regard, our surface-based method not only measures the diffusion values from narrow cortical fractions but also improves the sensitivity for detection by displaying the important reference values of the adjacent regions surrounding the abnormal cortex in a single surface (Figs. 10 and 11).

In addition, based on our study, further improvement can also be made in the interpretation of the diffusion data by using the specific patterns of diffusion abnormalities in each

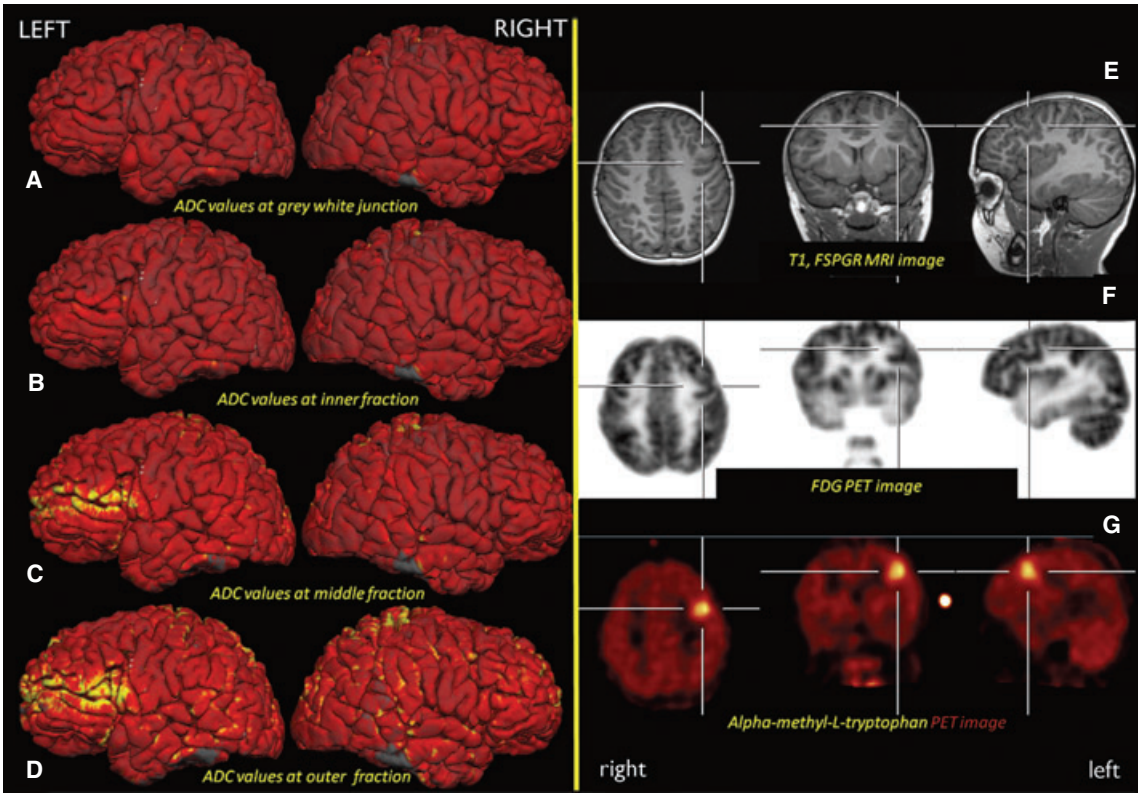

Figure 11.
Mean ADC values at different cortical fractions in a sample subject with intractable epilepsy prior to surgery. The MRI and the FDG PET findings were not helpful in localizing the epileptic focus. α-methyl-L-tryptophan (AMT) PET scan showed a focal increase in uptake on the left frontal cortex (**G**). Such focal uptake of AMT has been highly specific for identifying the epileptic focus and also has been associated with cortical dysplasia type IIB (with balloon cells) on histology (Chugani et al., 2011). Our surface-based analysis showed prominent diffusion abnormalities in the outer cortical fraction corresponding to the AMT PET findings. All surface images have same display scale.

of the cortical fractions and white matter layers. From our findings, a coefficient of the diffusion changes across layers to compare epileptic and normal regions can be used to estimate a prediction factor of epileptogenesis. Such an analysis would incorporate all the diffusion data from all the layers and provide an integrated output to compare all the regions of the epileptic brain. However, the values from such predication models would be reliable only if a sufficiently large number of subjects is used to estimate the coefficients. Nevertheless, we expect the relationship between the epileptic cortex and the expressed diffusion changes to be strong and helpful in identifying the epileptic cortex while minimizing the signal noise and measurement errors associated with this complex analysis.

Additional use in clinical practice

This surface-based method in addition to providing the diffusion values from narrow regions is likely to be also useful in evaluating the medial surface of the cortical hemisphere in cortex folded within the interhemispheric fissure. Furthermore, the diffusion values can also be extracted and displayed for the insular cortex, which lies deep inside the sylvian fissure. Epilepsy-related diffusion findings from these regions, which are difficult to sample with intracranial electrodes, would be of great benefit in the clinical setting.

Limitations by low spatial resolution

One of the methodologic concerns in our study is the limited spatial resolution of the diffusion images. This is a common limitation for diffusion images acquired in clinical settings. In our analysis, following the tensor calculation, the diffusion images were registered and resampled to a higher resolution (same as the structural image: $1 \times 1 \times 1$ mm). Such interpolation of the image will only provide a smoothed image with no addition of diffusion data. This common limitation prevails in most of the tractographic and voxel-based analyses (such as TBSS) studies

using such low-resolution diffusion images. Considering this limitation, we limited the fractionation of the cortical thickness to three layers with an average neocortical thickness of 3 mm. Our assumption was that three-layer fractionation might provide meaningful measurements at least a millimeter apart and without significant partial volume artifacts. Further improvement in the spatial resolution of the diffusion images will significantly improve the accuracy of our laminar analysis.

Effect of partial volume

In the present study, the partial volume effect from the CSF with high isotropic diffusivity can be suspected by a gradual increase in ADC values from the deeper regions to the superficial regions as would be expected (Fig. 4). A 7% increase in the mean ADC values was noted in the outer fraction compared to the middle fraction of the control subject's region. Similarly, in the electrographically normal region the increase was about 8.8%. These increases in mean ADC values (7–8.8%) in both the control regions (control subjects and electrographically normal cortex in epileptic subjects) can be attributed to the partial volume effect of the CSF. Proportionately, if we expect 7–8.8% increase in the mean ADC value due the CSF partial volume effect in the outer fraction, the remaining approximately 7.6% of the 15.5% increase might be attributed to the effect of epilepsy in the seizure-onset regions.

Similarly, the FA values were also seen decreasing in a somewhat linear fashion from deeper to superficial layers (Fig. 7). A consistent pattern of FA decrease of 12–16% was noted in all four fractions of epileptic subjects compared to the control subjects. There was no difference between the onset and electrographically normal regions in both the epileptic and control groups. From Figure 7, it can be noted that, even in this outer fraction, significant differences were detected between the epileptic and control groups (16%) to the same extent as for the middle (13.5%) and inner (13.3%) layers. Had the partial volume effect from CSF overwhelmed the diffusion measurements in this fraction, we might have observed homogeneous diffusion values (FA of CSF, which is close to zero) between the two groups. Therefore, the diffusion values measured in the outer fraction meaningfully represent the diffusion characteristics of the superficial cortex despite partial volume effects from the CSF. Because both the epileptic and control groups were analyzed in the same manner, any measurement errors due to partial volume effects must be the same for both groups, and hence our findings of differences in diffusivity could indeed be an underestimation of the actual diffusion abnormalities.

Segmentation and registration errors

In the method used for this study, the segmentation and registration steps are important and critical to the overall reliability of this analysis method. The segmentation of the gray and white matter and the delineation of the G-W and G-P surfaces effectively depend on signal contrast between the gray and white matter regions. In our study, we have used structural MR images experimentally tested to achieve free-geometrical distortion and maximize high gray–white contrast ratio (measured approximately > 2). All the subjects had normal clinical MRI findings with no obvious lesion or gray–white blurring. Poor gray–white contrast or presence of lesions (e.g., gray–white blurring) will affect the segmentation protocols. Future studies with acquisition protocols ideally optimized for high contrast between gray–white matter regions will further improve the accuracy of the segmentation procedure. In addition, future use of multiple structural images acquired during the clinical scans will also improve the segmentation procedure by reducing the signal-to-noise ratio and minimizing errors due to movement artifacts (Fischl et al., 2004; Reuter et al., 2010). In addition, since diffusion images are prone to spatial distortion, registration errors between the structural and diffusion scans are expected. In our study we used several corrective features to minimize this error. (1) We used the FA image, which has a signal profile (gray matter: darker, white matter: brighter signal) similar to the structural (T_1-weighted) image to perform the diffusion-to-structural registration. Using the images with a similar signal profile will improve the accuracy of the registration process. (2) We also performed the registration procedure prior to the segmentation of the structural image. Because segmentation of the structural image is particularly error prone in regions with blurring of G-W interface, using the unsegmented image avoids the unexpected deformation of the diffusion images during the nonlinear registration process. (3) Moreover, since both the structural and the diffusion images were acquired during the same clinical scanning session, gross spatial misalignments (related to head placement in the scanner) between the structural and diffusion scans are not expected. Nevertheless, in our study, we visually inspected all the images following this registration process to verify the lack of such misalignments.

In conclusion, our analysis suggests specific patterns of diffusion changes in the cortical fractions and the underlying white matter of the epileptic region compared to electrographically normal and normal control regions. The abnormal increase in ADC of the superficial cortex might be associated with microstructural abnormalities commonly seen in layers II through IV of epileptic cortex. Such combined use of a high-resolution structural image to extract the diffusion values that are highly sensitive to microstructural alterations would be of immense clinical use in localizing epileptogenic cortex.

Acknowledgment

This study is funded by NIH grants NS47550, NS64033 (to E.A), and NS064989 (to HTC).

Disclosure

None of the authors has any conflict of interest to disclose. We confirm that we have read the Journal's position on issues involved in ethical publication and affirm that this report is consistent with those guidelines.

References

Alkonyi B, Juhasz C, Muzik O, Asano E, Saporta A, Shah A, Chugani HT. (2009) Quantitative brain surface mapping of an electrophysiologic/metabolic mismatch in human neocortical epilepsy. *Epilepsy Res* 87: 77–87.

Asano E, Juhasz C, Shah A, Sood S, Chugani HT. (2009) Role of subdural electrocorticography in prediction of long-term seizure outcome in epilepsy surgery. *Brain* 132:1038–1047.

Beaulieu C. (2002) The basis of anisotropic water diffusion in the nervous system – a technical review. *NMR Biomed* 15:435–455.

Chugani HT, Kumar A, Kupsky W, Asano E, Sood S, Juhasz C. (2011) Clinical and histopathologic correlates of 11C-alpha-methyl-L-tryptophan (AMT) PET abnormalities in children with intractable epilepsy. *Epilepsia* 52:1692–1698.

Concha L, Beaulieu C, Gross DW. (2005) Bilateral limbic diffusion abnormalities in unilateral temporal lobe epilepsy. *Ann Neurol* 57:188–196.

Concha L, Beaulieu C, Wheatley BM, Gross DW. (2007) Bilateral white matter diffusion changes persist after epilepsy surgery. *Epilepsia* 48: 931–940.

Dale AM, Fischl B, Sereno MI. (1999) Cortical surface-based analysis. I. Segmentation and surface reconstruction. *Neuroimage* 9:179–194.

Duncan JS. (2008) Imaging the brain's highways-diffusion tensor imaging in epilepsy. *Epilepsy Curr* 8:85–89.

Duning T, Kellinghaus C, Mohammadi S, Schiffbauer H, Keller S, Ringelstein EB, Knecht S, Deppe M. (2010) Individual white matter fractional anisotropy analysis on patients with MRI negative partial epilepsy. *J Neurol Neurosurg Psychiatry* 81:136–139.

Engelhorn T, Weise J, Hammen T, Bluemcke I, Hufnagel A, Doerfler A. (2007) Early diffusion-weighted MRI predicts regional neuronal damage in generalized status epilepticus in rats treated with diazepam. *Neurosci Lett* 417:275–280.

Farrell MA, Vinters HV. (1997) General neuropathology of epilepsy. In Jerome Engel Jr, Pedley TA (Eds) *Epilepsy*. Lippincott-Raven, Philadelphia, PA, pp. 157–175.

Fischl B, Dale AM. (2000) Measuring the thickness of the human cerebral cortex from magnetic resonance images. *Proc Natl Acad Sci U S A* 97:11050–11055.

Fischl B, Sereno MI, Dale AM. (1999a) Cortical surface-based analysis. II: inflation, flattening, and a surface-based coordinate system. *Neuroimage* 9:195–207.

Fischl B, Sereno MI, Tootell RB, Dale AM. (1999b) High-resolution intersubject averaging and a coordinate system for the cortical surface. *Hum Brain Mapp* 8:272–284.

Fischl B, Salat DH, Busa E, Albert M, Dieterich M, Haselgrove C, van der Kouwe A, Killiany R, Kennedy D, Klaveness S, Montillo A, Makris N, Rosen B, Dale AM. (2002) Whole brain segmentation: automated labeling of neuroanatomical structures in the human brain. *Neuron* 33:341–355.

Fischl B, Salat DH, van der Kouwe AJ, Makris N, Segonne F, Quinn BT, Dale AM. (2004) Sequence-independent segmentation of magnetic resonance images. *Neuroimage* 23(Suppl. 1):S69–S84.

Garbelli R, Zucca I, Milesi G, Mastropietro A, D'Incerti L, Tassi L, Colombo N, Marras C, Villani F, Minati L, Spreafico R. (2011) Combined 7-T MRI and histopathologic study of normal and dysplastic samples from patients with TLE. *Neurology* 76:1177–1185.

Govindan RM, Makki MI, Sundaram SK, Juhasz C, Chugani HT. (2008) Diffusion tensor analysis of temporal and extra-temporal lobe tracts in temporal lobe epilepsy. *Epilepsy Res* 80:30–41.

Guye M, Ranjeva JP, Bartolomei F, Confort-Gouny S, McGonigal A, Regis J, Chauvel P, Cozzone PJ. (2007) What is the significance of interictal water diffusion changes in frontal lobe epilepsies? *Neuroimage* 35: 28–37.

Jiang H, van Zijl PC, Kim J, Pearlson GD, Mori S. (2006) DtiStudio: resource program for diffusion tensor computation and fiber bundle tracking. *Comput Methods Programs Biomed* 81:106–116.

Konermann S, Marks S, Ludwig T, Weber J, de Greiff A, Dorfler A, Leonhardt G, Wiedemayer H, Diener HC, Hufnagel A. (2003) Presurgical evaluation of epilepsy by brain diffusion: MR-detected effects of flumazenil on the epileptogenic focus. *Epilepsia* 44:399–407.

Moseley ME, Cohen Y, Kucharczyk J, Mintorovitch J, Asgari HS, Wendland MF, Tsuruda J, Norman D. (1990) Diffusion-weighted MR imaging of anisotropic water diffusion in cat central nervous system. *Radiology* 176:439–445.

Mukherjee P, Berman JI, Chung SW, Hess CP, Henry RG. (2008) Diffusion tensor MR imaging and fiber tractography: theoretic underpinnings. *AJNR Am J Neuroradiol* 29:632–641.

Reuter M, Rosas HD, Fischl B. (2010) Highly accurate inverse consistent registration: a robust approach. *Neuroimage* 53:1181–1196.

Roberts DW. (2011) Seizure-localizing value and functional implications of diffusion-based imaging in epilepsy. *World Neurosurg* 75:434–435.

Rugg-Gunn FJ, Eriksson SH, Symms MR, Barker GJ, Duncan JS. (2001) Diffusion tensor imaging of cryptogenic and acquired partial epilepsies. *Brain* 124:627–636.

Smiley JF, Konnova K, Bleiwas C. (2012) Cortical thickness, neuron density and size in the inferior parietal lobe in schizophrenia. *Schizophr Res* 136:43–50.

Smith SM. (2002) Fast robust automated brain extraction. *Hum Brain Mapp* 17:143–155.

Smith SM, Jenkinson M, Johansen-Berg H, Rueckert D, Nichols TE, Mackay CE, Watkins KE, Ciccarelli O, Cader MZ, Matthews PM, Behrens TE. (2006) Tract-based spatial statistics: voxelwise analysis of multi-subject diffusion data. *Neuroimage* 31:1487–1505.

Williams MR, Chaudhry R, Perera S, Pearce RK, Hirsch SR, Ansorge O, Thom M, Maier M. (2012) Changes in cortical thickness in the frontal lobes in schizophrenia are a result of thinning of pyramidal cell layers. *Eur Arch Psychiatry Clin Neurosci* 263:25–39.

Woermann FG, Sisodiya SM, Free SL, Duncan JS. (1998) Quantitative MRI in patients with idiopathic generalized epilepsy. Evidence of widespread cerebral structural changes. *Brain* 121(Pt 9):1661–1667.

Yu JT, Tan L. (2008) Diffusion-weighted magnetic resonance imaging demonstrates parenchymal pathophysiological changes in epilepsy. *Brain Res Rev* 59:34–41.